

Ultralight pion and superheavy baryon dark matterAzadeh Maleknejad*Theoretical Physics Department, CERN, 1211 Geneva 23, Switzerland*

Evan McDonough

Department of Physics, University of Winnipeg, Winnipeg, Manitoba R3B 2E9, Canada

(Received 14 July 2022; accepted 18 October 2022; published 9 November 2022)

We consider a dark confining gauge theory with millicharged ultralight pions (ULP) and heavy baryons as dark matter candidates. The model simultaneously realizes the ultralight (strongly interacting ultralight millicharged particle or “STUMP”) and superheavy (“WIMPzilla”) dark matter paradigms, connected by the confinement scale of the dark QCD. It is a realization of millicharged ultralight dark matter, unlike conventional axions, and exhibits a mass splitting between the charged and neutral pions. ULPs can easily provide the observed density of the dark matter, and be cosmologically stable, for a broad range of dark QCD scales and quark masses. The dark baryons, produced via gravitational particle production or via freeze-in, provide an additional contribution to the dark matter density. Dark matter halos and boson stars in this context are generically an admixture of the three pions and heavy baryons, leading to a diversity of density profiles. That opens up the accessible parameter space of the model compared with the standard millicharged dark matter scenarios and can be probed by future experiments. We briefly discuss additional interesting phenomenology, such as ULP electrodynamics, and cosmic ULP backgrounds.

DOI: [10.1103/PhysRevD.106.095011](https://doi.org/10.1103/PhysRevD.106.095011)**I. INTRODUCTION**

Few things are known with the degree of certainty that it is known dark matter exists: Cosmic microwave background (CMB) data, in the context of the Λ CDM cosmological model, indicate a nonzero abundance of dark matter to a statistical significance greater than 70σ [1]. However, beyond its gravitational influence, little is known about the identity of dark matter. Emblematic of our ignorance of dark matter is the mass of its constituent degrees of freedom, which could range from 10^{-22} eV to 10^{15} g.

Dark matter candidates in the sub-eV mass range are collectively known as ultralight dark matter (ULDM) [2]. In the decades since the advent of axion dark matter [3–5], this class of models has been populated with fuzzy [6,7], Bose-Einstein condensate [8], bosonic superfluid [9,10], fermionic superfluid [11,12], and superconducting, e.g., strongly interacting ultralight millicharged particle (STUMP) [13], dark matter candidates, among others. Axion dark matter is but the tip of the ULDM iceberg.

These models are in part compelling due to their potential for resolving small-scale tensions in the Λ CDM model, such

as the core-cusp problem, missing satellites, and galactic rotation curves [14–17]. However, the modern science case is broader and deeper than this alone (see [18] for a recent overview). ULDM exhibits a wide array of interesting phenomenology, such as vortices [19–22] and their imprints [23,24], electromagnetic signatures (e.g., [25], and see [26] for a review), gravitational waves [27–31], as well as in varied particle physics contexts, such as muon $g - 2$ experiments [32] and neutrino oscillation experiments [33]. This wide array of potential observables for both current and next generation experimental efforts motivates a thorough study of the ULDM model space.

In this paper we study the emergence of millicharged ULDM in the context of a confining gauge theory. We find that the pions of this theory, namely, ultralight pions (ULPs), are an excellent dark matter candidate. These are analogous to the Standard Model pions in their field theory formulation, but share important properties with the conventional axion, such as the cosmological evolution as a coherent field. ULPs are distinguished from a conventional axion in part by their characteristic spectrum: a neutral pion π^0 and charged pions π^\pm . The masses of the pions are dictated by the confinement scale, the quark mass, and the charges of the quarks. As a concrete example, we consider the possibility that the dark quarks have a small electric charge. While so-called millicharged dark matter has been widely explored, this is the first electrically millicharged ULDM candidate (for 1 eV to 10 keV millicharged DM

Published by the American Physical Society under the terms of the Creative Commons Attribution 4.0 International license. Further distribution of this work must maintain attribution to the author(s) and the published article's title, journal citation, and DOI. Funded by SCOAP³.

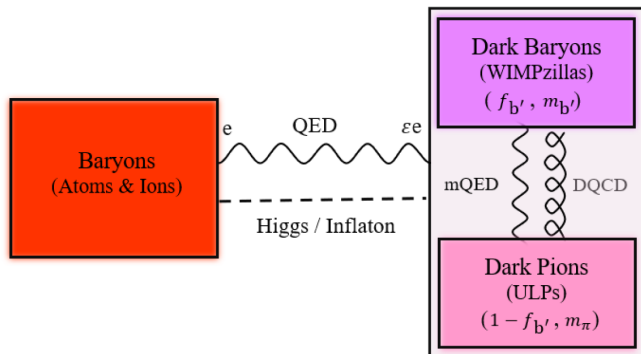


FIG. 1. Taxonomy of the ULP-WIMPzilla model. Dark matter is composed of ultralight pions (ULPs) and superheavy dark baryons, with masses m_{π} and m_b jointly determined by the confinement scale and quark mass, constituting a fraction of the dark matter $f_{b'}$ and $f_{\pi} = 1 - f_{b'}$, respectively. The ULPS and WIMPzillas interact with each other through the dark strong force (DQCD) and visible electromagnetism by their millicharges $\epsilon\epsilon$ (mQED). They also interact with the Standard Model electromagnetically as well as gravitationally, through the Higgs, or via the inflaton.

models see [34]). ULPs are a close cousin of the STUMP model proposed in [13] and provide an alternative model realization of STUMPs.

The ULPs themselves are but the tip of another iceberg, composed of the mesonic and hadronic states of the theory. For concreteness we focus on a dark sector similar to quantum chromodynamics (QCD); namely, we consider an $SU(3)$ gauge theory with two flavors of light quark, which we refer to as dark QCD (see Fig. 1). For past works on dark QCD, see, e.g., [35–37]. In our setup, the lightest baryons, namely, a dark proton and a dark neutron, are stable and themselves can be excellent dark matter candidates. The dark baryons are naturally in the realm of WIMPzillas [38–41], also known as superheavy dark matter, since the dark baryon mass is anchored to the confinement scale, which is in turn related to the pion decay constant, which is $\gtrsim 10^{10}$ GeV in order to realize ULPs as a dark matter candidate. See Fig. 2.

Superheavy dark matter has its own rich phenomenology [42], and disentangling superheavy DM candidates, e.g., spin-0, spin-1/2, spin-1 [43], spin-3/2 [44], and spin-s [45],

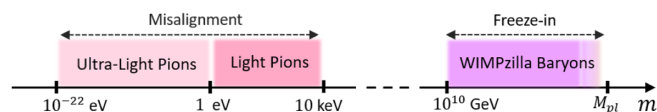


FIG. 2. Summary of dark matter production mechanisms with respect to mass. This setup predicts an admixture of light dark pions (Sec. III A) and superheavy baryons (Sec. III B) as the cold dark matter. Light and ultralight pions are produced via the misalignment mechanics in the early universe. The baryon WIMPzillas can be generated gravitationally or via freeze-in mechanism by an inflaton portal, Higgs portal, and millicharged QED interactions.

is an interesting direction for future work. In the ULP model, the superheavy dark matter is a fermion, and itself a composite state. This setup has a very rich phenomenology which is specified in terms of three unknown scales, i.e., mass of the dark quarks, scale of the dark confinement, and scale of inflation. The focus of current work is at the limit where the dark confinement happens before inflation. The exhaustive study of the setup throughout the parameters will be presented in [46].

The outline of this paper is as follows: in Sec. II we introduce our dark QCD theory and the spectrum of particles in the confined phase. In Sec. III we develop ULPs as a dark matter candidate, along with their superheavy dark baryons. In Sec. IV we find approximate solutions to ULP boson stars and fuzzy ULP halos. We conclude in Sec. VI with a discussion of other directions for ULP detection, in particular, by utilizing their interactions with the photon. The details of the calculation of the number density of heavy dark baryons is presented in Appendix.

Notation.—The dark $SU(N)_x$ gauge field and its quarks are denoted as \mathbf{X}_{μ} and χ , respectively. The SM Higgs doublet is denoted as H and B_{μ} is the SM's $U(1)_Y$ hypercharge. Throughout this work, unless otherwise specified, by “quark,” “pion,” “baryon,” “eta-prime,” and “glueball,” refer to dark sector components. Here (π^0, π^+, π^-) are the dark pions, η' is the dark eta-prime, and (b, n) denote the dark baryons. The dark baryon number is shown as B' . The Hubble parameter is shown as H . Finally, to avoid confusion with the SM baryon density, we used $\Omega_{b'}$ and $f_{b'}$ for the relic density and fraction of energy in the dark baryons.

II. EFFECTIVE FIELD THEORY AND COSMOLOGICAL HISTORY OF DARK QCD

We consider a confining dark gauge symmetry $SU(N)_x$ coupled to two dark quarks (“up” and “down”) in the fundamental representation of the dark color $SU(N)_x$ as

$$\mathcal{L}_X = i\bar{\chi}\not{D}\chi - \mathbf{m}_{\chi}\bar{\chi}\chi - \frac{1}{2}\text{Tr}\mathbf{X}_{\mu\nu}\mathbf{X}^{\mu\nu}, \quad (1)$$

where $\not{D} = \not{\partial} - ig_x\not{X}$, in which $\mathbf{m}_{\chi} = \text{diag}(m_u, m_d)$ is a quark mass matrix. The quarks $\chi_{u,d}$ carry dark baryon numbers as $b'_u = b'_d = \frac{1}{3}$. We are interested in the limit that m_{χ} is negligible compared to the confinement scale of the $SU(N)_x$, i.e., $m_{\chi} \ll \Lambda_x$. The theory Eq. (1) then has an approximate $SU(2)_L \times SU(2)_R \times U(1)_V \times U(1)_A$ chiral symmetry, under which $\chi_{L,R}$ transforms as a doublet.

At energy scales below the confinement scale of $SU(N)_x$, the dark QCD (“DQCD”) vacuum spontaneously breaks the $SU(2)_L \times SU(2)_R$ global symmetry down to the diagonal subgroup $SU(2)_V$, via the x -quark-antiquark condensate as

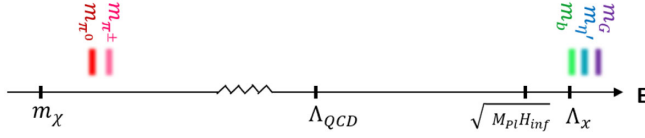


FIG. 3. Mass spectrum of the theory. The dark baryon and η' masses are around Λ_x , and the lightest scalar glueball mass is $m_G \approx 6\Lambda_x$. The neutral pion mass is $m_{\pi^0} \approx \sqrt{m_\chi \Lambda_x}$ that for very light quarks $m_{\pi^0} \ll \Lambda_x$. The mass splitting between charged and neutral pions is $\frac{m_{\pi^\pm}^2 - m_{\pi^0}^2}{m_{\pi^0}^2} \sim e^2 \frac{e^2 F_\pi}{m_u + m_d}$.

$$\langle \bar{\chi}_i^L \chi_j^R \rangle = V^3 \delta_{ij}, \quad i, j \in \{u, d\}, \quad (2)$$

where $V \sim \Lambda_x^3$. The quarks are then confined into mesons and hadrons. We have two composite pseudoscalar states,

$$\boldsymbol{\pi} = \pi^a \boldsymbol{\tau}_a, \quad \eta', \quad (3)$$

where $\boldsymbol{\tau}_a$ are the generators of the $SU(2)$ algebra, the $SU(2)$ triplets $\boldsymbol{\pi}$ are Nambu-Goldstone bosons (NGBs) corresponding to spontaneous symmetry breaking of $SU(2)_A$, and η' is a massive singlet, which are all their own antiparticles. There is additionally a spectrum of mesons and baryons, just as in standard visible QCD. However, unlike QCD, here there is no analog of the electroweak interactions, which makes the pions stable.

The mass spectrum of the lowest-lying mesonic and hadronic states is shown in Fig. 3. Before studying the spectrum of the theory in detail, we first consider ways in which dark QCD may be coupled to the visible Standard Model.

A. Portals to the Standard Model

Any dark sector is unavoidably coupled to the SM gravitationally. Besides, there are numerous portals of dark QCD to the standard model (see, e.g., [47]). For example, the quarks of the dark sector might be connected to the SM via a small “milli-” charge under SM hypercharge, or through a coupling to the SM Higgs. In particular, the dark quarks may have a very small hypercharge, i.e.,

$$\not{D} = \not{\partial} - ig_x \not{X} - i\epsilon_{u,d} e \not{B}, \quad (4)$$

where e is the electric charge, B_μ is the SM hypercharge, and $\epsilon_{u,d} \ll 1$ are two very small numbers. For millicharged dark sectors as extensions of the Standard Model embedded in unifying gauge framework see [48].

To this end we consider two types of scenarios as shown in Table I. We label as Type I the case in which the up and down quarks have equal but opposite hypercharges, and we label as Type II the case in which, analogous to the SM quarks, the dark quarks have charges $+(2/3)\epsilon e$ and $-(1/3)\epsilon e$. In both cases, there is an electrically neutral

TABLE I. We consider two types of millicharged dark quarks parametrized in terms of the dimensionless parameter $\epsilon \ll 1$.

	ϵ_u	ϵ_d
Type I	$+\frac{1}{2}\epsilon$	$-\frac{1}{2}\epsilon$
Type II	$+\frac{2}{3}\epsilon$	$-\frac{1}{3}\epsilon$

pion and two electrically charged pions π^\pm with charge $\pm e\epsilon$. In Type I there is an electrically neutral neutron and electrically charged proton, while in Type II both the neutron and the proton are charged. (See Fig. 4.)

A second possibility is a Higgs portal to the Standard Model. For example, the dark quarks can be directly coupled to the SM Higgs via a dimension-five operator $\mathcal{L}_{\chi-H} = \sum_{i=u,d} \frac{y_i}{\Lambda_H} \mathbf{H}^\dagger \mathbf{H} \bar{\chi}_i \chi_i$, where \mathbf{H} is the SM Higgs doublet and Λ_H is the mass of the heavy mediator between DM and Higgs. In the confining phase, this interaction generates effective couplings of the Higgs to both the mesons and the baryons. A variation on this is to consider portals of the confined phase, and in particular consider *dark-baryon-philic* couplings of the Standard Model, analogous to leptophilic dark matter [49] and leptophobic dark matter [50]. Dark-baryon-philic interactions can emerge from simple UV completions, e.g., in models such as [51,52] wherein the global $U(1)$ dark baryon number is promoted to a spontaneously broken gauge symmetry, as proposed in [13].

An additional possibility is to couple the dark sector to the SM indirectly, i.e., through an inflaton portal. This could again take the form of a baryon-philic coupling, or couplings to the full spectrum of the confined phase.

B. The spectrum

We now consider the spectrum of composite states in the confining phase of dark QCD. Among the composite states, we will see that the pions and baryons are stable while η' and glueballs are unstable and short-lived.

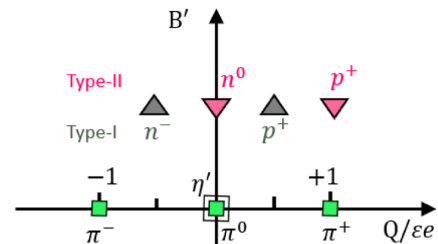


FIG. 4. Composite states in charge-baryon number plane. Based on the charge type of the dark quarks in Table I, dark baryons have different charges. In Type I, neutrons and protons have $\pm \frac{1}{2}\epsilon e$ electric charges, respectively, while in Type II neutrons are neutral and protons have $+\epsilon e$ charge.

1. Pions

The dynamics of the pions in the confined phase is well described by chiral perturbation theory [53]. In this framework, confinement can be described as a spontaneous symmetry breaking of a composite field Σ_{ij} , with additional terms that explicitly break the $SU(2)_A$ global symmetry. The action can be expressed as

$$S_\Sigma = \int dx^4 \sqrt{-g} \left(\text{Tr}[D_\mu \Sigma]^2 + m^2 |\Sigma|^2 - \frac{\lambda}{4} |\Sigma|^4 \right) + \mathcal{L}_{\chi\text{PT}}, \quad (5)$$

where $D_\mu \Sigma$ is the covariant derivative defined as

$$D_\mu \Sigma = \partial_\mu \Sigma - ieA_\mu (\mathbf{Q}\Sigma - \Sigma\mathbf{Q}), \quad \mathbf{Q} = \text{diag}(\varepsilon_u, \varepsilon_d), \quad (6)$$

and $\mathcal{L}_{\chi\text{PT}}$ denotes terms that explicitly break the global chiral symmetry.

In the symmetry-broken phase, Σ_{ij} can be expanded around its vacuum as

$$\Sigma_{ij} = \frac{F_\pi + \sigma(x)}{\sqrt{2}} \exp\left(\frac{2i\pi^a(x)\tau_a}{F_\pi}\right), \quad (7)$$

where $\langle \Sigma \rangle = \frac{F_\pi}{\sqrt{2}} \text{diag}(1, 1)$ is the vacuum solution. The effective action of the pions is then determined by $\mathcal{L}_{\chi\text{PT}}$, which, at leading order, is given by

$$\mathcal{L}_{\chi\text{PT}} = \text{Tr}[\Sigma^\dagger m_\chi + m_\chi^\dagger \Sigma] + \dots \quad (8)$$

Moreover, the most generic χPT can have a term as [54,55]

$$\mathcal{L}'_{\chi\text{PT}} = if(\eta') \text{Tr}[\Sigma^\dagger m_\chi - m_\chi^\dagger \Sigma], \quad (9)$$

where $f(\eta')$ is an odd function of η' . Although η' is not a true Goldstone boson due to the axial $U(1)_A$ anomaly of the strong interactions, it combines with the pions via the above effective interaction.

In the case of neutral and degenerate-mass quarks, the effective action of the pions takes an exceptionally simple form as

$$\mathcal{L}_\pi|_{m_u=m_d} = \frac{1}{2} \left(\text{Tr} \partial_\mu \boldsymbol{\pi} \partial^\mu \boldsymbol{\pi} + m_u V^3 \text{Tr} \cos\left(\frac{\boldsymbol{\pi}}{F_\pi}\right) \right), \quad (10)$$

in strong resemblance to a conventional axion.

More generally, expanding to quadratic order in the pions, we find

$$\mathcal{L}_\pi = \frac{1}{2} \partial_\mu \pi^0 \partial^\mu \pi^0 + D_\mu \pi^+ D^\mu \pi^- - \frac{m_{\pi^0}^2}{2} \pi^{02} - m_{\pi^\pm}^2 \pi^+ \pi^- + \mathcal{L}_{\pi\gamma}, \quad (11)$$

where the mass of pions is given by the Gell-Mann-Oakes-Renner relation

$$m_{\pi^0}^2 = \frac{V^3}{F_\pi^2} (m_u + m_d), \quad (12)$$

for the neutral pion, where $F_\pi \sim V \sim \Lambda_\chi$, and

$$m_{\pi^\pm}^2 = m_{\pi^0}^2 + 2\xi e^2 F_\pi^2 (\varepsilon_u - \varepsilon_d)^2, \quad (13)$$

for the charged pions, where the last term is the electromagnetic contribution to the mass splitting of $\pi^\pm - \pi^0$, and ξ is an order one parameter that should be fit by data. Therefore, given that $\varepsilon_u \sim -\varepsilon_d = \varepsilon$, $\xi = \mathcal{O}(1)$, and $F_\pi \sim V$, we have the mass splitting

$$\frac{m_{\pi^\pm}^2 - m_{\pi^0}^2}{m_{\pi^0}^2} \sim e^2 \frac{\varepsilon^2 F_\pi}{m_u + m_d}, \quad (14)$$

which, depending on ε , F_π , and the quark mass m_χ , can range from negligibly small to very large.

The pions are also coupled to the SM photon. The pion-photon interaction $\mathcal{L}_{\pi\gamma}$ in Eq. (11) is the chiral anomaly of the $U(1)_A$ via the triangle diagram of the massive charged baryons as [56]

$$\mathcal{L}_{\pi\gamma} = \sum_{b_i} Q_{b_i}^2 \frac{N_c}{8\pi^2 F_\pi} \pi^0 F \tilde{F}, \quad (15)$$

where N_c is the number of colors and $\sum_{b_i} Q_{b_i}^2 = A e^2 e^2$ is the charge of baryons inside the triangle loop where $A = 1/2$ ($A = 1$) in Type I (Type II). The pions also inherit quartic self-interactions and couplings coming both from the expansion of the cosine potential and from higher-order terms in chiral perturbation theory.

The coupling to the photon allows the neutral pion to decay as $\pi^0 \rightarrow \gamma\gamma$. Taking the $m_{\pi^0} \ll m_b$ limit, this decay rate can be written as

$$\Gamma(\pi^0 \rightarrow \gamma\gamma) = \frac{A\alpha_e^2 \varepsilon^4 \lambda^2 m_{\pi^0}^3}{64\pi^3 m_b^2} = \frac{A\alpha_e^2 \varepsilon^4 m_{\pi^0}^3}{64\pi^3 F_\pi^2}. \quad (16)$$

Therefore, the lifetime of π^0 in Type I is twice the lifetime of π^0 in Type II. Assuming $m_u \sim m_d = m_\chi$ and given that $m_{\pi^0}^2 \sim m_\chi \Lambda_\chi$, we find

$$\Gamma(\pi^0 \rightarrow \gamma\gamma) \sim \frac{2A\alpha_e^2}{64\pi^3} \varepsilon^4 m_\chi \left(\frac{m_\chi}{\Lambda_\chi}\right)^{\frac{1}{2}}. \quad (17)$$

For the π^0 to be long lived enough and a DM candidate, its lifetime should be longer than the age of the universe, $\Gamma = \hbar/\tau_U < \hbar/(4 \times 10^{17} \text{ s})$. This can be translated to the condition

$$\left(\frac{\varepsilon}{10^{-8}}\right)^4 \left(\frac{100 \text{ MeV}}{\Lambda_x}\right)^{\frac{1}{2}} \left(\frac{m_\chi}{0.1 \text{ MeV}}\right)^{\frac{3}{2}} < \frac{3}{2}. \quad (18)$$

Therefore, the pions can be made stable through any or all of a high confinement scale Λ , a small quark mass m_χ , or a small millicharge ε .

2. η' Meson

Similar to SM QCD, the global $U(1)_A$ symmetry of our dark QCD is broken by instantons. The mode associated with the $U(1)_A$ is the η' meson, which receives its mass due to the explicit breaking of $U(1)_A$ by the $SU(N)_x$ instantons as

$$V(\eta') = \Lambda_x^4 \cos\left(\frac{\eta'}{F_{\eta'}}\right), \quad (19)$$

where $F_{\eta'} \simeq \Lambda_x$ is the decay constant of η' . This endows the η' with a mass $m_{\eta'} \sim \Lambda_x$, which is parametrically heavier than the pions. The effective Lagrangian of the η' can be written as

$$\begin{aligned} \mathcal{L}_{\eta'} = & \frac{1}{2} \partial_\mu \eta' \partial_\mu \eta' + \Lambda_x^4 \cos\left(\frac{\eta'}{F_{\eta'}}\right) - \frac{\alpha_{\eta'\gamma}}{4\pi} \frac{\eta'}{F_{\eta'}} F_{\mu\nu} \tilde{F}^{\mu\nu} \\ & + \alpha_{\eta'\pi} |m_u - m_d| \eta' \pi^0 \vec{\pi} \cdot \vec{\pi}, \end{aligned} \quad (20)$$

where $\alpha_{\eta'\pi}$ and $\alpha_{\eta'\gamma}$ are two constants that should be given by the simulation. Note that the last term is isospin symmetry violating and hence is proportional to $|m_u - m_d|$.

The dark η' is unstable, just as in SM QCD. The decay channels of the η' are the decay to two photons, i.e., $\eta' \rightarrow \gamma\gamma$, as well as decay to three pions, i.e., $\eta' \rightarrow \pi^+ \pi^- \pi^0$ and $\eta' \rightarrow \pi^0 \pi^0 \pi^0$. The decay rate of η' to two photons can be estimated in terms of the same process in the SM as

$$\Gamma(\eta' \rightarrow \gamma\gamma) \approx \varepsilon^4 \left(\frac{m_{\eta'}}{m_{\eta'_{\text{SM}}}}\right)^3 \Gamma(\eta'_{\text{SM}} \rightarrow \gamma\gamma). \quad (21)$$

The $\eta'_{\text{SM}} \rightarrow \gamma\gamma$ is the dominate decay channel of η'_{SM} which specifies its lifetime as short as $\tau_{\eta'_{\text{SM}}} \approx 3 \times 10^{-21}$ s. In the η' case, we have

$$\Gamma(\eta' \rightarrow \gamma\gamma) \approx \frac{1}{10^{-2} \text{ s}} \left(\frac{\varepsilon}{10^{-13}}\right)^4 \left(\frac{m_{\eta'}}{10^{10} \text{ GeV}}\right)^3, \quad (22)$$

making the η' unstable on cosmological timescales. Meanwhile the decay rate of η' to three pions is given as

$$\Gamma(\eta' \rightarrow \pi\pi\pi) = \frac{\alpha_{\eta'\pi}^2 (m_u - m_d)^2}{64(2\pi)^3} m_{\eta'}, \quad (23)$$

which can be cosmologically fast or slow, depending on the mass splitting of the quarks, the η' -pion coupling, and

the mass of the η' . Given these two decay channels, the generic expectation is that any initial η' population should be unstable and decay to photons and pions.

3. Glueballs

In addition to the mesons and baryons, one expects that gluons can also form colorless states, called glueballs [57]. In that case, dark glueballs (DG) can form below the confinement scale as pure gluonic states. The properties of the glueballs in Yang-Mills have been studied in lattice gauge theory [58–62]. Their spectrum can be entirely parametrized by the confinement scale of the theory, or equivalently lightest glueball mass, $m_G \sim 6\Lambda_x$. The full QCD (including quarks), however, is more complicated and an active experimental and theoretical area of research. The lightest DG (denoted as G) is a scalar with quantum numbers $J^{PC} = 0^{++}$, and its effective Lagrangian can be written as

$$\mathcal{L}_G = \frac{1}{2} \partial_\mu G \partial_\mu G + \frac{1}{2} m_G^2 G^2 + f_3 G^3 + f_4 G^4, \quad (24)$$

where m_G is the mass and f_3 and f_4 are the self-couplings. The glueballs can be stable or decay through a variety of portals to the mesons. Given that G is a singlet under chiral symmetry, the DG-meson interactions are [63]

$$\mathcal{L}_{G\Sigma} = (g_1 F_\pi G + g_2 G^2) \text{Tr}[\Sigma^\dagger \Sigma], \quad (25)$$

which leads to a G and pion interaction term as

$$\mathcal{L}_{G\pi} \simeq \frac{\theta m_G^2}{2F_\pi} G \pi^2, \quad (26)$$

where $\theta = \frac{g_1 F_\pi^2}{(m_G^2 - m_\pi^2)}$ and its value should be given by the data. Therefore, the scalar DG decays into pions with the decay rate

$$\Gamma(G \rightarrow \pi^a \pi^a) = \frac{3\theta^2}{32\pi} \left(\frac{m_G}{F_\pi}\right)^2 \sqrt{m_G^2 - m_\pi^2}. \quad (27)$$

Assuming that the θ is $O(1)$, we have

$$\Gamma(G \rightarrow \pi^a \pi^a) \sim 10\Lambda_x, \quad (28)$$

which implies that DGs are unstable and very short-lived. As a result, the dark glueballs have no cosmological effect in this setup. For a similar framework in a different part of parameter space with cosmological relevant glueballs see [37,64].

4. Dark baryons

The lightest dark baryons are $p = uud$ and $n = ddu$ with masses $m_p \simeq m_n \approx N_x \Lambda_x$. Both baryons are stable,

even in the charged case, since there are no electrons or neutrinos in the model, and the dark baryon number is conserved. The dark baryons therefore serve as a potential dark matter candidate. For $\Lambda_x \gg \text{GeV}$, this falls in the category of superheavy dark matter (recently reviewed in [42]), and in particular, superheavy dark fermions. These baryons are feebly coupled to the SM and can only get generated via the freeze-in mechanism in the early universe, or else gravitationally. We defer a discussion of the primordial production of baryons to Sec. III.

III. DARK MATTER

We now focus our attention on the dark matter problem, namely, obtaining the observed relic density of cosmologically stable cold collisionless dark matter. As discussed above, the stable composite states in our model are the pions and the baryons. Here we consider these individually.

A. Pion dark matter: Light and ultralight

As a simple cosmological history, we consider that confinement occurs at a high scale Λ_x , above the scale of cosmic inflation. Similar to the conventional axion vacuum misalignment mechanism, the pion fields are each initialized with an initial value comparable to the pion decay constant. The phase of cosmic inflation serves to both homogenize the pion fields, and redshift away any thermal relics from the confining phase transition.

To constitute the observed dark matter, we demand the dark pions satisfy the following requirements:

- (1) Ultralight and light: We are interested in ULPs, $m_{\pi^a} < 1 \text{ eV}$, and light pions, $m_{\pi^a} = (1 \text{ eV} - 10 \text{ keV})$. They are generated via the misalignment mechanism in the early universe.
- (2) Stability: In our dark QCD, with neutral quarks, the pions are stable, since there are no electroweak interactions. In the millicharged case, this requires Eq. (18) to be satisfied.
- (3) Relic density: The three pions together constitute the observed dark matter density. The present day pion abundance is given by

$$\Omega_\pi = \frac{1}{6} (9\Omega_r)^{3/4} \frac{F_\pi^2}{M_{\text{pl}}^2} \sum_{a=0,\pm} \left(\frac{m_{\pi^a}}{H_0} \right)^{1/2} \theta_{\pi^a}^2 \quad (29)$$

in analogy to the usual axion case [65].

- (4) Isocurvature modes: Light pions pick up isocurvature perturbations during inflation, which is strongly constrained by the CMB [66]. Assuming that $\theta_{\pi^a} \sim \pi$, this leads to an upper bound on the scale of inflation, as

$$\frac{H_{\text{inf}}}{M_{\text{pl}}} \lesssim 8.8 \times 10^{-5} \frac{\Omega_{\text{DM}} F_\pi}{\Omega_{\pi^a} M_{\text{pl}}}. \quad (30)$$

Finally the requirement that the dark matter be collisionless is satisfied due to the fact that the pion self-interactions and couplings are suppressed by the decay constant F_π , and additionally by the requirement that the millicharge be small enough to extend the pion lifetime to greater than the age of the universe. In the following, we discuss the parameter space of dark pions. (See the left panel of Fig. 5.)

1. Ultralight pions

The dark pions with masses $m_\pi < 1 \text{ eV}$ evolve as a coherent scalar field. Similar to Axion-like particles, this implies the ULPs evolve as cold pressureless dark matter in the late universe, when each ULP field oscillates in the minimum of its potential. Demanding that the pions constitute an $\mathcal{O}(1)$ fraction of the observed dark matter density enforces a lower bound on the pion decay constant, and hence the dark QCD scale, given by $F_\pi > 8.8 \times 10^{10} \text{ GeV}$. From these considerations, and the relation $m_{\pi^0}^2 \sim m_\chi \Lambda_x$, we may deduce the mass range for the dark quarks, as

$$m_\chi < 5 \times 10^{-20} \text{ eV}. \quad (31)$$

Further demanding that the charged pions, with mass given by Eq. (13), remain in the ultralight regime, $m_\pm < \text{eV}$, puts an upper bound on the charge of the dark quarks as

$$\epsilon e < \frac{1 \text{ eV}}{F_\pi}. \quad (32)$$

Curiously, the mass bound Eq. (31) is within a few orders of magnitude of the benchmark fuzzy dark matter mass. For the purposes of this work, we do not consider the fine-tuning of the dark quark mass to be any more concerning of a problem than it already is for bosonic ultralight DM (e.g., axion or fuzzy DM).

2. Light pions

The light dark pions have masses in the interval $m_{\pi^a} = (1 \text{ eV} - 10 \text{ keV})$. Using $H_0 \approx 2 \times 10^{-33} \text{ eV}$ in Eq. (29), we have

$$\Omega_{\pi^a} \approx 0.25 \left(\frac{F_\pi}{8.8 \times 10^{10} \text{ GeV}} \right)^2 \left(\frac{m_{\pi^a}}{1 \text{ eV}} \right)^{\frac{1}{2}} \left(\frac{\theta_a}{\pi} \right)^2. \quad (33)$$

Demanding that the light dark pions made all the dark matter today gives

$$F_\pi \geq 8.8 \times 10^9 \text{ GeV}. \quad (34)$$

Therefore, our dark sector with light pions has heavy baryons with mass,

$$m_b \gtrsim 10^{10} \text{ GeV}. \quad (35)$$

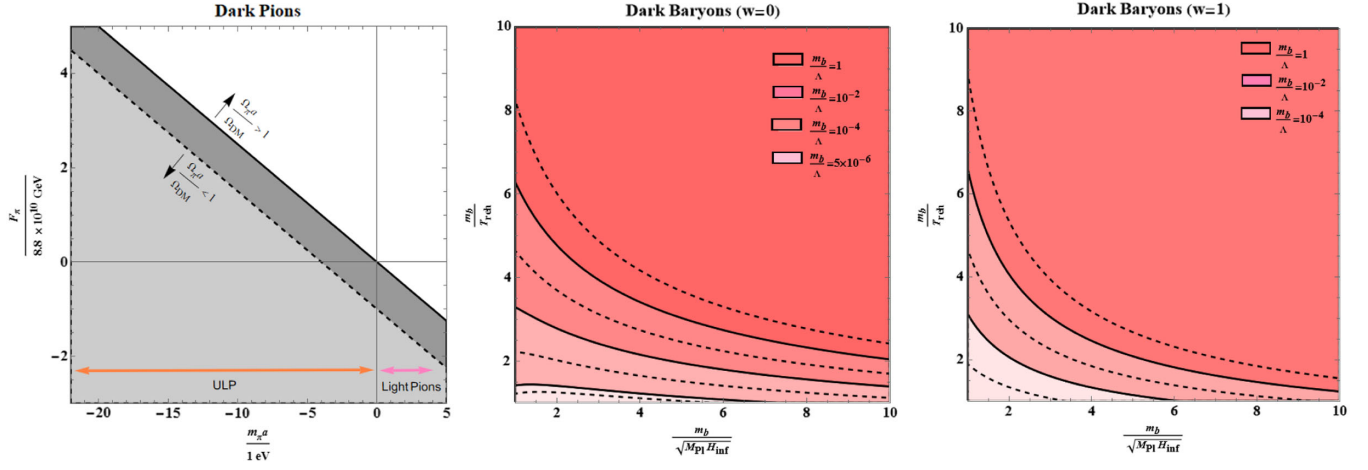


FIG. 5. The admixture of dark pions–WIMPzilla baryons with respect to parameters of the model, for freeze-in production of dark baryons (see Fig. 7 for gravitational production). Left panel: Accessible parameter space for the pions produced by the misalignment mechanism where the misalignment angles are $\theta_i \approx \pi$. The shaded region shows parameters corresponding to $\Omega_{\pi^a}/\Omega_{\text{DM}} \lesssim 1$, and the dashed line marked shows $\Omega_{\pi^a}/\Omega_{\text{DM}} = 10^{-2}$. Middle and right panels: Freeze-in production of baryons [by Higgs portal Eq. (39), inflaton portal Eq. (45), and QED portal Fig. 6] for the preheating phase with $w = 0$ (middle panel), and $w = 1$ (right panel). The parameter Λ denotes Λ_H/y for the Higgs portal case, $\sqrt{2}\Lambda_\phi/\lambda$ in the inflaton portal case, and $13.7m_b/e$ for the freeze-in via millicharged case. Each shaded region represents part of the parameter space with $\Omega_{b'}/\Omega_{\text{DM}} \lesssim 1$ for the given value of $\frac{m_b}{\Lambda}$. The dashed lines inside each shaded area make $\Omega_{b'}/\Omega_{\text{DM}} = 10^{-2}$.

Moreover, the mass and millicharge of the quarks can be on one of the following ranges:

$$1.1 \times 10^{-20} \text{ eV} \leq m_\chi \leq 1.1 \times 10^{-11} \text{ eV} \quad \text{and} \quad \epsilon e < \frac{1 \text{ eV}}{F_\pi},$$

which put an extremely tight upper bound on the charge as $\epsilon e < 10^{-19}$, or

$$m_\chi \leq 1.1 \times 10^{-20} \text{ eV} \quad \text{and} \quad \frac{1 \text{ eV}}{F_\pi} < \epsilon e < \frac{10^4 \text{ eV}}{F_\pi},$$

which demands $\epsilon e < 10^{-14}$.

B. Baryon WIMPzillas

The dark QCD we consider also allows for stable dark baryons. These may be produced gravitationally at the end of inflation, or else through freeze-in production via their interactions with the SM. Here we consider and study three different freeze-in mechanisms, i.e., inflaton portal freeze-in, Higgs portal freeze-in, and millicharged QED freeze-in. We summarize these different possibilities in Fig. 2.

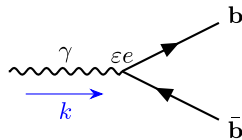


FIG. 6. The millicharged QED (mQED) portal of the charged dark baryons.

Gravitational production of the WIMPzillas is shown in Fig. 7.

At this point we need to further specify the thermal evolution of the universe and in particular the reheating phase that follows cosmic inflation. For the sake of generality, we consider the following phenomenological reheating model:

$$\rho_{\text{reh}} = \delta_{\text{reh}} \left(\frac{a_{\text{inf}}}{a_{\text{reh}}} \right)^4 \rho_{\text{inf}}, \quad (36)$$

where $\rho_{\text{inf}} = 3M_{\text{pl}}^2 H_{\text{inf}}^2$ is the inflation energy density, $\delta_{\text{reh}} \approx (a_{\text{reh}}/a_{\text{inf}})^{-(3w-1)}$ is the efficiency of the reheating

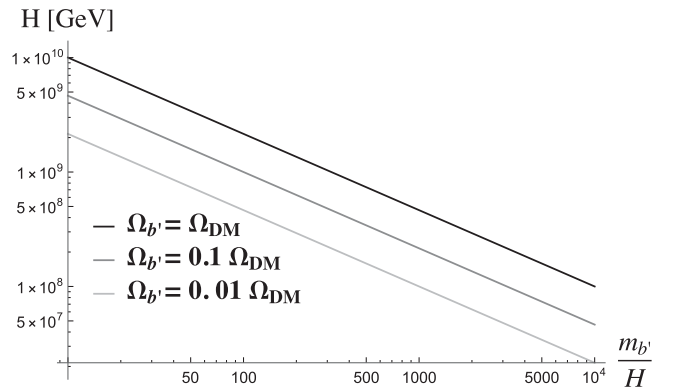


FIG. 7. Gravitational production of dark baryons WIMPzillas. The black, gray, and light gray lines correspond to 100%, 10%, and 1% of the observed dark matter in gravitationally produced dark baryons.

process, and w is the effective equation of state in the intermediate period between the end of inflation and the formation of the thermal bath. In the case that the inflaton oscillates coherently about the minimum of the potential, its energy density redshifts as matter, i.e., $w = 0$ with a $\delta_{\text{ref}} > 1$. On the other hand, if inflation ends with domination of the kinetic term, i.e., $w = 1$, we have $\delta_{\text{ref}} < 1$. The reheating energy density is $\rho_{\text{reh}} = \frac{\pi^2}{30} g_* T_{\text{reh}}^4$. The temperature after reheating scales as $T \propto 1/a$, while between the end of inflation until reheating it scales differently and at the beginning it scales as [67]

$$T(a) \approx \left(\frac{a_{\text{inf}}}{a} \right)^{\frac{3}{8}(1+w)} T_{\text{max}}, \quad (37)$$

where $a_{\text{inf}} < a < a_{\text{reh}}$ and T_{max} is

$$T_{\text{max}} \approx 0.2 \left(\frac{100}{g_{\text{eff}}} \right)^{\frac{1}{8}} \rho_{\text{inf}}^{\frac{1}{8}} T_{\text{reh}}^{\frac{1}{2}}. \quad (38)$$

1. Higgs portal

The dark baryons can be coupled to the SM Higgs as

$$\mathcal{L}_{\text{H}} = \frac{y}{\Lambda_{\text{H}}} \mathbf{H}^\dagger \mathbf{H} \sum_{i=p,n} \bar{b}_i b_i, \quad (39)$$

where we approximately take $m_p \approx m_n$ and $y = y_b \approx y_n$. This interaction can arise either from SM Higgs–dark quark interaction $\mathcal{L} \propto |H|^2 \bar{\chi} \chi$ or by dark-baryon-philic interactions, e.g., in a scenario with a gauged baryon number [51]. The latter case leaves the pion mass unchanged and only contributes to the baryon mass. In contrast, in the former case, after the electroweak phase transition, the coupling Higgs makes generates an effective mass for the dark pions as $m_{\pi^0} \sim 246 \left(\frac{y \Lambda_x}{\Lambda_{\text{H}}} \right)^{\frac{1}{2}}$ GeV, which, in the region of interest for freeze-in production, generically lifts the ULPs out of the ultralight regime. For simplicity, here we treat the pion mass independently from the Higgs-baryon coupling.

At temperatures above the Electroweak (EW) symmetry breaking scale and $\Lambda_x > T_{\text{reh}}$, the thermally averaged annihilation cross section of dark fermions with mass m_b is $\langle \sigma_{\text{H}} v \rangle \approx \frac{1}{8\pi} \frac{y^2}{\Lambda_{\text{H}}^2} \frac{3T}{m_b}$ [67]. The decay rate of the dark baryons associated with the Higgs interaction is

$$\Gamma_{\text{H}} = \frac{3T}{(2\pi)^{\frac{3}{2}}} \left(\frac{yT}{\Lambda_{\text{H}}} \right)^2 \left(\frac{m_b}{T} \right)^{\frac{1}{2}} e^{-m_b/T}. \quad (40)$$

Demanding that the WIMPzillas are never in thermal equilibrium with the SM, we find

$$y^{-1} \Lambda_{\text{H}} \gg \frac{1}{(2\pi)^{\frac{3}{2}}} \left(\frac{m_b}{T_{\text{max}}} \right)^{\frac{1}{4}} e^{\frac{m_b}{2T_{\text{max}}}} \sqrt{M_{\text{pl}} T_{\text{max}}}. \quad (41)$$

For typical values of $m_b \sim 10^{10}$ GeV, $m_b/T_{\text{max}} \sim 10$, and $y \sim 0.1$, it gives $\Lambda \sim 10^{14}$ GeV.

This interaction generates a relic density of dark baryons via the freeze-in mechanism. Details of the calculations are provided in Appendix, and here we only report the final results. Concretely, the relic density of the dark baryons produced through the Higgs portal is [see Eq. (A9)]

$$\Omega_{b'} h^2 \simeq \mathcal{A} \left(\frac{y m_b}{\Lambda_{\text{H}}} \right)^2 \frac{\exp[10(3 - \alpha\beta^{\frac{1}{2}})]}{\beta^{4/(1+w)-1/2}}, \quad (42)$$

where α and β are

$$\alpha \equiv \frac{m_b}{\sqrt{H_{\text{inf}} M_{\text{pl}}}} \quad \text{and} \quad \beta \equiv \frac{\sqrt{H_{\text{inf}} M_{\text{pl}}}}{T_{\text{reh}}}, \quad (43)$$

which are both more than one and $\mathcal{A} = \frac{(10\pi^2)^{-w/(1+w)}}{2(1+w)}$. We have $\mathcal{A} = 1/2$ for $w = 0$ and $\mathcal{A} = 3/2 \times 10^{-2}$ for $w = 1$.

The abundance of dark baryons as a function of model parameters is shown in Fig. 5, in the plane of m_b/T_{reh} and $m_b/\sqrt{M_{\text{pl}} H_{\text{inf}}}$, with the value of coupling y indicated by background color. Dashed lines indicate 1% of the dark matter in dark baryons while solid lines indicate 100%. Regions below the dashed and above the solid lines correspond to intermediate fractions between 1% and 100%. From this one may appreciate that, given values for any two of these parameter combinations, one may tune the dark baryon abundance by varying the third. We define the fraction of dark matter that this process produces as

$$f_{b'} \equiv \frac{\Omega_{b'}}{\Omega_{\text{DM}}}, \quad (44)$$

which may easily range from 0 to 1. This is illustrated in Fig. 5.

2. Inflaton portal

We now consider a direct coupling of the dark baryons to the inflaton field, as

$$\mathcal{L}_{\text{inf}} = \frac{\lambda}{\Lambda_{\text{inf}}} \phi^2 \sum_{i=p,n} \bar{b}_i b_i, \quad (45)$$

where we approximately take $\lambda = \lambda_b \approx \lambda_n$. We consider an inflaton potential dominated by a quadratic term after inflation

$$V(\phi) \simeq \frac{1}{2} m_\phi^2 \phi^2. \quad (46)$$

Demanding that the dark baryons are never in thermal equilibrium gives

$$\lambda^{-1} \Lambda_{\text{inf}} \gg \frac{1}{\sqrt{2}(2\pi)^{\frac{3}{2}}} \left(\frac{m_b}{T_{\text{max}}} \right)^{\frac{1}{4}} e^{\frac{m_b}{2T_{\text{max}}}} \sqrt{M_{\text{pl}} T_{\text{max}}}. \quad (47)$$

Assuming for simplicity that $m_b \gg T_{\text{max}} \gg m_\phi$, and following the same procedure as for the Higgs portal, we find

$$\Omega_{b'} \approx \frac{1}{2} \mathcal{A} \left(\frac{\lambda m_b}{\Lambda_{\text{inf}}} \right)^2 \frac{\exp[10(3 - \alpha\beta^{\frac{1}{2}})]}{\beta^{4/(1+w)-1/2}}, \quad (48)$$

where \mathcal{A} , α , and β are defined as in the Higgs portal case. The fraction of dark matter that the inflaton portal can produce is again $f_{b'} = [0, 1]$, which is illustrated in Fig. 5.

3. Millicharged QED

The dominant electromagnetic processes between the dark baryons and electromagnetic plasma are

$$\bar{f}f \rightarrow \bar{b}b \quad \text{and} \quad \gamma^* \rightarrow \bar{b}b, \quad (49)$$

which are proportional to ε^2 , f denotes SM charged fermions, and γ^* denotes plasmons. The other possible process is $\gamma\gamma \rightarrow \bar{b}b$ which is proportional to ε^4 and highly suppressed. The decay rate of dark baryons associated with the mQED processes is

$$\Gamma_{em} = \frac{3\varepsilon^2 \alpha_{em}^2}{(2\pi)^{\frac{3}{2}}} T \left(\frac{T}{m_b} \right)^{\frac{3}{2}} e^{-m_b/T}. \quad (50)$$

We demand that the WIMPzillas are never in thermal equilibrium with the SM. This puts an upper bound on the millicharge as

$$\varepsilon \ll 4 \times 10^2 \left(\frac{m_b}{M_{\text{pl}}} \right)^{\frac{1}{2}} \left(\frac{m_b}{T_{\text{max}}} \right)^{\frac{1}{4}} e^{\frac{1}{2}m_b/T_{\text{max}}}. \quad (51)$$

Given that $m_b \gtrsim 10^{10}$ GeV and $m_b > T_{\text{max}}$, this condition is satisfied throughout the parameter space for $\varepsilon \lesssim 10^{-2}$.

The relic density of the heavy dark baryons produced today through freeze-in by QED processes is

$$\Omega_{b'} h^2 \simeq 10^{-2} \mathcal{A} \varepsilon^2 \left(\frac{\varepsilon \alpha_{em}}{10^{-2}} \right)^2 \frac{\exp[10(3 - \alpha\beta^{\frac{1}{2}})]}{\beta^{4/(1+w)-1/2}}, \quad (52)$$

where $\alpha_{em} = e^2/4\pi$ and \mathcal{A} , α , and β are similar to (52) (see Fig. 5). Figure 5 implies that generating a significant fraction of dark baryons from the mQED interactions requires $\varepsilon \gtrsim 10^{-4}$. As we discuss later in Sec. V, this possibility is ruled out by constraints on the millicharge of the light pions.

4. Gravitational production

Finally, dark baryons may be produced gravitationally, without relying on any direct coupling to the Standard Model or the inflaton. So-called ‘‘gravitational particle production’’ [38–41,68] is generated by the nonadiabatic expansion of spacetime that occurs at the end of inflation. See [42] for a recent review.

In our work we assume that the dark QCD theory is in the confining phase during inflation and reheating, and hence $m_b \gg H$. Gravitational production in this parameter regime has been extensively studied in recent years [69–73]. In particular, the dark matter density in the regime $H \ll m_b$, with $m_b \lesssim m_\phi$, with m_ϕ the mass of the inflaton, is given by [73]

$$\frac{\rho_b}{s} \simeq 4 \times 10^{-10} \text{ GeV } \mathcal{C} \left(\frac{m_b}{10^9 \text{ GeV}} \right) \left(\frac{H}{10^9 \text{ GeV}} \right) \quad (53)$$

$$\times \left(\frac{T_{\text{re}}}{10^{10} \text{ GeV}} \right) \left(\frac{m_b}{m_\phi} \right)^2, \quad (54)$$

where $\mathcal{C} = 10^{-2} - 10^{-3}$ is a numerical constant and s is the entropy density. This may be compared to the observed DM abundance $\rho_{\text{DM}}/s \sim 4 \times 10^{-10}$ GeV. As a fiducial example, we fix $m_\phi = 10^{13}$ GeV and $T_{\text{re}} = 10^{11}$ GeV. The dark matter abundance, as a function of H and the ratio m_b/H is shown in Fig. 7. In this figure the black line denotes parameters such that $\Omega_{b'}$ gives 100% of the observed dark matter abundance, while the gray and light gray lines correspond to 10% and 1% of the dark matter, respectively.

IV. ULP HALOS AND BOSON STARS

We now consider cosmological and astrophysical implications of our model. A striking feature of ultralight bosonic dark matter candidates is the existence of self-gravitating soliton solutions. In the context of fuzzy dark matter, with $m \sim 10^{-22}$ eV, these solitons are on cosmological scales, forming the core of dark matter halos. For larger masses, such as the benchmark QCD axion mass $m \sim 10^{-5}$ eV, the soliton solutions instead correspond to boson stars, which have their own signatures, such as gravitational waves. In both cases, the soliton solutions can be described in terms of the wave function, corresponding to the nonrelativistic limit of the scalar field. The resulting equations of motion are Schrödinger and Poisson equations. For a discussion of the allowed mass range and constraints, see [74].

We seek to construct such soliton solutions in the context of ULP dark matter. To do so, we first decompose the charged pions π_\pm into real components, as

$$\pi^\pm = \pi^1 \pm i\pi^2, \quad (55)$$

and take the nonrelativistic limit of $\pi^{0,1,2}$ as

$$\pi^i = \frac{1}{\sqrt{2m_i}} [\psi_i e^{-im_i t} + \psi_i^* e^{im_i t}], \quad (56)$$

with $i = 0, 1, 2$. The equations of motion of the system are then given by three copies of the Schrödinger equation,

$$i\hbar \frac{\partial \psi_i}{\partial t} = -\frac{\hbar^2}{2m_i} \nabla^2 \psi_i + m_i \Phi \psi_i, \quad (57)$$

coupled via the Poisson equation,

$$\nabla^2 \Phi = 4\pi G \sum_{i=0,1,2} m_i |\psi_i|^2, \quad (58)$$

where $m_{1,2} \equiv m_{\pm}$. For simplicity we have neglected non-gravitational interactions of the pions, which are suppressed by the pion decay constant. We leave this interesting aspect to future work.

To construct soliton solutions, we follow Refs. [75–77]. Assuming an ansatz for the spatial dependence of the pion wave functions [75]

$$\psi_i(x) = \sqrt{\frac{3N_i}{\pi^3 R_i^3}} \operatorname{sech}\left(\frac{r}{R_i}\right), \quad (59)$$

the Hamiltonian of the system may be straightforwardly derived as [77]

$$H = \sum_{i=1}^3 \left[a \frac{N_i}{m_i R_i^2} + b \frac{m_i^2 N_i^2}{R_i} \right] + \sqrt{2b} \sum_{\substack{i,j=1 \\ i \neq j}}^3 \frac{m_i m_j N_i N_j}{\sqrt{R_i^2 + R_j^2}}, \quad (60)$$

which generalizes the expression of [77] from two to three axions, but specializes to the sech ansatz of [75]. The constants a and b are ansatz dependent, and for the sech ansatz are given by [75]

$$a = \frac{12 + \pi^2}{6\pi^2}, \quad b = \frac{6}{\pi^4} (12\zeta(3) - \pi^2). \quad (61)$$

Finally, following [75] we work in dimensionless variables, defined by the rescalings given in [75].

We note that a general solution for the pion wave functions will correspond to a soliton with a net electric charge. For simplicity, we focus on solutions that are electrically neutral. The charge of a soliton may be expressed as

$$Q = 4\epsilon e \int d^3x (\hat{\pi}_1 \pi_2 - \hat{\pi}_2 \pi_1), \quad (62)$$

where we have decomposed the standard relation for a charged complex scalar field into the real scalar components. An electrically neutral soliton corresponds to one of

three cases: $\pi_1 = \pi_2$, $\pi_1 = 0$, or $\pi_2 = 0$. We consider the case $\pi_1 = \pi_2$, and hence $\psi_1 = \psi_2$.

To find an approximate ground state solution, building on the procedure of [77], we vary the Hamiltonian with respect to the radii R_i , while holding fixed both the total mass of the halo and the relative fraction of the mass contained within each dark matter component. We fix the total mass

$$M_{\text{tot}} = \sum_{i=1}^3 M_i, \quad (63)$$

where

$$M_i \equiv m_i N_i = m_i \int d^3r |\psi_i(r)|^2. \quad (64)$$

We also fix the relative fraction of the mass in each component,

$$f_i = \frac{N_i}{N_{\text{tot}}}. \quad (65)$$

One may reasonably expect that f_i depends on the local environment of dark matter solitons, and on the primordial abundances of the ULPs. In this sense, varying f_i corresponds to accounting for the diversity of dark matter halos.

Soliton solutions for varying f_i are given in the left panel of Fig. 8, where we consider the simple case that $m_{\pm} = 3m_0$. In all cases we explicitly confirm that the Hessian of the Hamiltonian is positive definite, and thus the solutions are stable. We consider four fiducial example solitons, corresponding to a purely π^0 halo, and halos with 5%, 20%, and 100% of the mass contained in π^{\pm} . One may easily appreciate that by adjusting the fraction of dark matter in the charged vs neutral pions, the central density becomes higher and the core radius smaller. This effect becomes more dramatic as the ratio of pion masses is made larger. While we restrict ourselves here to a mild mass hierarchy, we note this is made partly for illustrative purposes, and additionally so that the nonrelativistic limit may be consistently applied to both fields.

The impact of raising the charged pion mass is shown in the right panel of Fig. 8, where we fix the charged pions to be 5% of the mass of the halo and adjust the charged pion mass. For larger values of the charged pion mass, a distinct soliton is present at small radii, with a density that is orders of magnitude larger than the outer edges of the density profile.

The diversity of ULP soliton density profiles is particularly interesting given the mild tension between the diversity of observed halos [78] and the predicted universal properties of fuzzy dark matter solitons; see, e.g., [74,79,80] for a discussion and constraints. In the ULP model, a diversity of halos naturally emerges from adjusting the mixture of pions

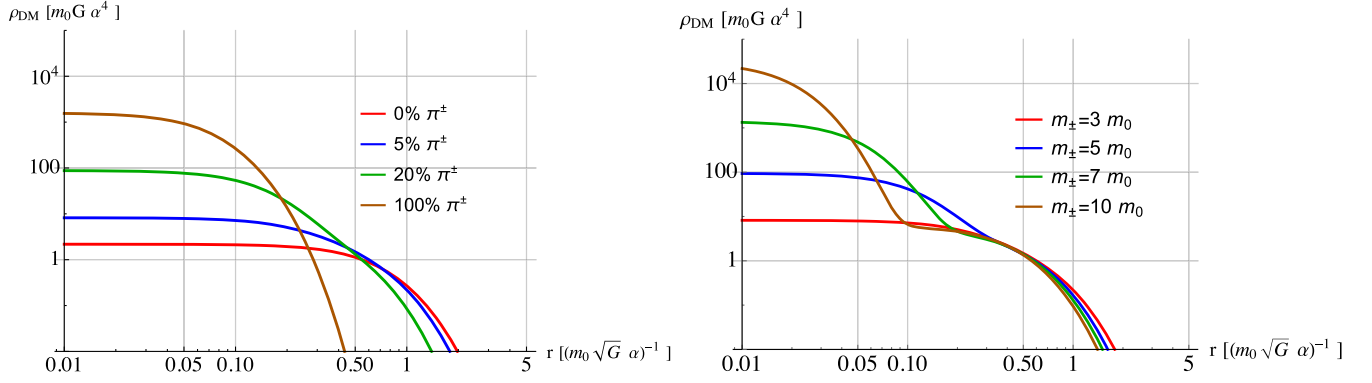


FIG. 8. Soliton solutions to self-gravitating ULPs in the nonrelativistic limit. All solutions have the same total mass, $M \equiv \sum_i m_i \int d^3r |\psi_i(r)|^2$. The units are defined with respect to an arbitrary energy scale α (when self-interactions are included, this scale is fixed to be the decay constant [75]). Left panel: We fix mass ratio $m_{\pm}/m_0 = 3$ and vary the fraction of the mass of the soliton composed of π_{\pm} . As the fraction increases, the soliton contracts and the central density grows larger. Right panel: We fix the mass fraction $f_{\pm} = 5\%$ and vary the mass ratio m_{\pm}/m_0 . As the mass ratio grows larger, a distinct high-density inner soliton emerges at small radii. In all cases we have fixed the total mass of the halo.

that make up the dark matter halo. In the case of a large high hierarchy, e.g., if π^0 is in the fuzzy range while π^{\pm} is in the conventional QCD axion range, dark matter halos can be expected to range from an Navarro–Frenk–White profile to the cored halos familiar from fuzzy dark matter.

V. CURRENT CONSTRAINTS AND AVENUES FOR DETECTION

In this section, we discuss the current constraints and the possibility of detection of the millicharged particles (MCP), as well as the dark QCD phase transition, and ULPs more generally.

A. Bounds on millicharge

The constraints on light MCPs are very strong. In Table II we summarize the current astrophysical, cosmological, and laboratory bounds on MCPs with $m_{\text{MCP}} \lesssim 1$ MeV. Some of these constraints can be avoided in our setup, as indicated in the last column of the table. The strongest bound on MCP dark matter comes from CMB, leading to the constraint [81–83]

$$\varepsilon < 10^{-15} \left(\frac{m}{\text{eV}} \right). \quad (66)$$

This constraint can be avoided in our setup once the fraction of the DM density in the charged pions is less than 0.4%, i.e., $f_{\pi^{\pm}} < 0.1$, or if the charged pion mass is in the ultralight regime. (It is noteworthy to mention that CMB constraints on millicharged coherent scalars, e.g., $m < 1$ eV, have never been worked out, and we defer to future work.) Note this still leaves open the possibility of ULPs comprising 100% of the dark matter, with $f_{\pi^0} \gtrsim 0.996$. As a result, the allowed parameter space for our charged pions is greatly enlarged compared to the

standard scenario of MCP dark matter. The strongest bound on the millicharge that cannot be avoided comes from the stellar cooling that gives [84,85]

$$\varepsilon < 1.7 \times 10^{-14}. \quad (67)$$

Several scenarios are proposed in the literature to evade the stellar bounds. For details see [86] and the references therein. The millicharged dark pions also interact with the SM baryons. The Rutherford-type scattering cross section of the pions off of a SM proton through a photon is

$$\sigma_{\pi^{\pm}b} \sim \frac{\alpha_{em}^2 \varepsilon^2}{\mu^2 v_{\text{rel}}^4}, \quad (68)$$

where v_{rel} is its relative velocity and $\mu \approx m_{\pi^{\pm}}$ is the SM proton and dark pions reduced mass. That gives an upper bound on the charge as $\varepsilon < 10^{-15} (\frac{m}{\text{eV}})$ [34,87]. For detailed discussion of the phenomenology and detection possibility of generic light millicharged dark matter see [34]. The parameter space of our setup, therefore, is divided into two parts:

- (i) charged pions make more than 0.4% of the dark matter with millicharge $\varepsilon < 10^{-15} (\frac{m_{\pi^{\pm}}}{\text{eV}})$,
- (ii) charge pions make a subdominant part of the dark matter, i.e., $f_{\pi^{\pm}} < 0.004$, with millicharge $\varepsilon < 1.7 \times 10^{-14}$.

B. Detection of millicharge

The main approach to detect light millicharged particles is the direct deflection method [81]. This experiment is based on distorting the local dark matter flow with time-varying fields and measuring these distortions with shielded resonant detectors. The expected reach of the direct deflection experiment is MCPs in the range 1–10⁷ eV and charge

TABLE II. The current (astrophysical, cosmological, and laboratory) constraints on MCPs with $m_{\text{MCP}} \lesssim 1$ MeV, such as light and ultralight pions. (For possible proposed mechanisms to evade stellar bounds see [86] and the references therein.) The column “avoidance” refers to the region of parameter space where the constraint of that row does not apply. Here f_π denotes the fraction of dark matter, not the decay constant.

	Method	Constraint on ϵ	Reference	Avoidance
Astrophysics	Supernova cooling	$10^{-9} < \epsilon < 10^{-7}$	[84]	
	Stellar cooling	$\epsilon < 1.7 \times 10^{-14}$	[84,85]	
	Solar cooling	$\epsilon < 10^{-13.6}$	[88]	
	Magnetars	$e^2 \left(\frac{m}{\text{eV}}\right) < 10^{-16}$	[89]	
	Milky Way satellites	$\epsilon < 10^{-15} \left(\frac{m}{\text{eV}}\right)$	[34,87]	$f_{\pi^\pm} < 10\%$
Cosmology	BBN	$\epsilon < 2.1 \times 10^{-9}$	[84,90,91]	
	CMB	$\epsilon \lesssim 2 \times 10^{-12} \left(\frac{m}{\text{keV}}\right)$	[81–83]	$f_{\pi^\pm} < 0.4\%$
	SZ effect	$\epsilon < 2 \times 10^{-9}$	[92]	$m_{\pi^\pm} \gg 10^{-7}$ eV
	SN dimming	$\epsilon < 4 \times 10^{-9}$	[93]	$m_{\pi^\pm} \gg 10^{-7}$ eV
	Pulsar timing and FRBs	$\epsilon \left(\frac{eV}{m}\right) < 10^{-8}$	[94]	$f_{\pi^\pm} < 10\%$
Laboratory	Laser experiments	$\epsilon < 3 \times 10^{-6}$	[93]	
	Lamb shift	$\epsilon < 10^{-4}$	[95]	
	Positronium	$\epsilon < 3.4 \times 10^{-5}$	[96]	
	Coulomb’s law deviations	$\epsilon \lesssim 5 \times 10^{-6}$	[97]	$m_{\pi^\pm} \gg 1$ eV
	Schwinger effect in cavities	$\epsilon \lesssim 10^{-6}$	[98]	$m_{\pi^\pm} \gg 1$ eV

in the range $\epsilon = 10^{-16} - 10^{-9}$ which can be improved by 1 order of magnitude in the long-term project [34,81]. This can be used to search for pions in the “light” range, i.e., $m_\pi = [1 \text{ eV}, 10 \text{ keV}]$.

C. Detection of dark QCD phase transition

If the dark QCD phase transition is first order, it can produce gravitational waves background with the frequency peak $f \gtrsim 10^4$ Hz. Such frequencies are above the LIGO/Virgo band and in the range of ultra-high-frequency gravitational waves. For a recent review on several detector concepts that have been proposed to detect these ultrahigh frequency signals see [99].

D. Other directions for ULP discovery

Analogous to axion electrodynamics, the ULP model exhibits *ULP-electrodynamics*. This is described by the Lagrangian

$$\mathcal{L}_{\text{ULP-EM}} = \mathcal{L}_\pi + \frac{1}{4} F^2 + e^2 e^2 \pi^+ \pi^- A_\mu A^\mu + g \frac{\pi^0}{4F_\pi} F\tilde{F}, \quad (69)$$

where \mathcal{L}_π corresponds to the mass and kinetic terms of the ULPs. From this one may derive the modified vacuum Maxwell equations as

$$\begin{aligned} \vec{\nabla} \cdot \vec{E} &= \frac{g}{F_\pi} \vec{B} \cdot \vec{\nabla} \pi^0 - e^2 e^2 \pi^+ \pi^- V, \\ \vec{\nabla} \times \vec{B} - \frac{\partial E}{\partial t} &= \frac{g}{F_\pi} \left(\vec{E} \times \vec{\nabla} \pi^0 - \vec{B} \frac{\partial \pi^0}{\partial t} \right) - e^2 e^2 \pi^+ \pi^- \vec{A}. \end{aligned} \quad (70)$$

We defer to future work an exploration of the ULP signal for axion detection experiments such as ADMX [100]. One might also search for these interactions in the form of “Cosmic ULP backgrounds,” analogous to the recently proposed cosmic axion background [101], but with one cosmic background for each ULP. Also in a cosmological context, the coupling of photons to the charged pions may be an additional source of resonant production of the former. The equation of motion for a Fourier mode of the photon field A^μ , with wave number k and polarization \pm , in an Friedmann–Lemaître–Robertson–Walker space-time, is given by

$$A''_{k\pm} + \left(k^2 + e^2 e^2 \pi^+ \pi^- \pm \frac{g}{F_\pi} k \pi^{0'} \right) A_{k\pm} = 0, \quad (71)$$

where $'$ denotes a derivative with respect to conformal time. This differs from the more conventional axion case (see, e.g., [102]) by the masslike coupling to the charged pions. The latter provides an additional mechanism for parametric resonance production of photons, as has been studied in an axion context in, e.g., [103].

VI. DISCUSSION

In this work we have developed the theory of ULP dark matter and dark baryon WIMPzillas, which together comprise the ULP-WIMPzilla model. In this model, ultralight dark matter arises as composite states of a confining gauge theory, namely, the Goldstone bosons of chiral symmetry breaking, analogous to the Standard Model pions. In the limit of very small dark quark masses, $m_q \lesssim 10^{-19}$ eV, and

high confinement scale $\Lambda_x \gtrsim 10^{10}$ GeV, the dark pions enjoy an axionlike cosmological history and can provide the observed abundance of dark matter. The mass spectrum of pions encodes the charge and confinement scale of the dark QCD-like theory, and is in turn encoded in the density profile of dark matter halos (or boson stars, depending on the mass of the pions).

As the name would suggest, the pions themselves are only part of the ULP-WIMPzilla model. There are additional degrees of freedom in the theory which may exhibit interesting dynamics, such as the dark baryons. Because of the high confinement scale, the dark baryons naturally realize the WIMPzilla paradigm. Produced either gravitationally or via freeze-in, the dark baryons can constitute a small to significant fraction of the dark matter for a wide range of parameters.

There are a few things worth highlighting before closing this article:

- (1) The ULP-WIMPzilla model is the first scenario of ultralight ($m < \text{eV}$) dark matter in a confining gauge theory, and the first example of an electrically millicharged ultralight ($m < \text{eV}$) dark matter candidate. The related but distinct mass range $m = [\text{eV}, 10 \text{ keV}]$ is studied in [34].
- (2) ULPs are the first model of three ultralight scalars, building on previous work on two ultralight scalars [76,77]. The ULP model predicts two of the three scalars are degenerate in mass, and predicts a mass splitting with the third set by the millicharge.
- (3) The ULP-WIMPzilla model is the first scenario to unify ultralight and fermionic WIMPzilla dark matter, with the two components unavoidably connected by common underlying parameters. Dark matter is generically an admixture of neutral pions, charged pions, and baryon WIMPzillas. This leads to a diversity of dark matter halos.
- (4) Depending on the millicharge, the quark mass, and confinement scale, the charged pions may have a mass comparable to the neutral pion or may be much heavier. In the latter case, the neutral pion can be wavelike (or “fuzzy”) while the charged pions may be wavelike or particlelike. Charged pions with $m_{\pi^\pm} > 10 \text{ keV}$ exhibit their own phenomenology, which we defer to future work.
- (5) The strongest constraint on the light millicharge by CMB is alleviated if the charged pions are a subdominant component of the dark matter, $f_{\pi^\pm} < 0.4\%$. This is independent of the fraction of DM in the neutral pions or dark baryons. This significantly opens up the parameter space of the model, while being testable at future experiments. The ultralight scalar with $m < 1 \text{ eV}$ behaves as a coherent state, and the CMB constraints on that case have never been worked out. We leave this effect to future work.

Finally, we address an important question: how can ULPs, and their UV completion in dark QCD, be distinguished experimentally from a conventional axion model, with a UV completion in scalar fields, and which is devoid of strong interactions? The suggestion presented in this work is to perform a dedicated search for the whole structure of the theory, namely, the ULP-WIMPzilla model, its pattern of charges and masses, and the associated phenomenology (such as gravitational waves from the dark QCD phase transition). This proposal sidesteps a related but distinct question: given a detection at ADMX or related axion search, how may we test the nature of the axion as fundamental or composite? We leave this interesting question to future work.

ACKNOWLEDGMENTS

The authors thank Cora Dvorkin, Wayne Hu, Eiichiro Komatsu, Joachim Kopp, and Matthew McCullough for discussions and comments. E. M. is supported in part by a Discovery Grant from the National Science and Engineering Research Council of Canada.

APPENDIX: NUMBER DENSITY OF HEAVY DARK BARYONS

This appendix presents the calculations of heavy fermion generation by a Higgs portal of the form Eq. (39). Here we followed the analysis performed in [67]. At temperatures above the EW symmetry breaking ($T > 100 \text{ GeV}$), the Higgs field includes two states, i.e., $\mathbf{H} = \begin{pmatrix} \text{H}^+ \\ \text{H}^0 \end{pmatrix}$, and hence there are two annihilation channels to dark baryons

$$\text{H}^0\text{H}^0 \rightarrow \bar{b}_x b_x \quad \text{and} \quad \text{H}^+\text{H}^- \rightarrow \bar{b}_x b_x. \quad (\text{A1})$$

Because of the isospin symmetry, the matrix elements of these two channels are equivalent, and the final thermally averaged cross section is doubled. The thermally averaged annihilation cross section is

$$\begin{aligned} \langle \sigma_{\text{H}v} \rangle &= \frac{4^2}{n_{\text{eq}} n_{\text{eq}}} \int \frac{d^3 \vec{p}_1}{(2\pi)^3} \int \frac{d^3 \vec{p}_2}{(2\pi)^3} \bar{\sigma}_{\text{H}^{\dagger}\text{H} \rightarrow \bar{b}_x b_x} v_{\text{M}\ddot{a}}(p_1, p_2) \\ &\times \exp(-(E_1 + E_2)/T), \end{aligned} \quad (\text{A2})$$

where $\bar{\sigma}_{\text{H}^{\dagger}\text{H} \rightarrow \bar{b}_x b_x}$ is the spin-averaged annihilation cross section and $v_{\text{M}\ddot{a}}(p_1, p_2)$ is the Møller velocity

$$v_{\text{M}\ddot{a}}(p_1, p_2) = \sqrt{|\vec{v}_1 - \vec{v}_2|^2 - |\vec{v}_1 \times \vec{v}_2|^2}, \quad (\text{A3})$$

where $\vec{v} = \vec{P}/E$. Since $\bar{\sigma}_{\text{H}^{\dagger}\text{H} \rightarrow \bar{b}_x b_x}$ is a function of s only, Eq. (A4) can be further simplified as [67]

$$\langle \sigma_{Hv} \rangle = \frac{4^2}{n_{\text{eq}} n_{\text{eq}}} \frac{T}{32\pi^4} \int_{4m_b^2}^{\infty} ds \sqrt{s} (s - 4m_b^2) K_1 \left(\frac{\sqrt{s}}{T} \right) \times \bar{\sigma}_{H^\dagger H \rightarrow \bar{b}_x b_x}(s), \quad (\text{A4})$$

where $s = (p_1 + p_2)^2$, K_1 is the modified Bessel function of the second kind of order 1, and $\bar{\sigma}_{H^\dagger H \rightarrow \bar{b}_x b_x}$ is the cross section associated with the Higgs annihilation

$$\bar{\sigma}_{H^\dagger H \rightarrow \bar{b}_x b_x}(s) = \frac{1}{32\pi} \frac{\lambda^2}{\Lambda_H^2} \frac{1}{s} \sqrt{s - 4m_b^2} \sqrt{s - 4m_H^2}. \quad (\text{A5})$$

In the limit that $m_b \gg T$, the thermally averaged annihilation cross section of dark fermions with mass m is [67]

$$\langle \sigma_{Hv} \rangle \approx \frac{1}{8\pi} \frac{\lambda^2}{\Lambda_H^2} \frac{3T}{m_b}. \quad (\text{A6})$$

The number density of dark baryons generated by the SM Higgs is

$$n_b(t) = a^{-3}(t) \int_{a_{\text{inf}}}^{a(t)} \frac{d \ln a}{H} a^3 \langle \Gamma_H \rangle n_{\text{eq}} \approx \frac{4/(2\pi)^4}{(1+w)} \left(\frac{a_{\text{inf}}}{a(t)} \right)^3 \left(\frac{\lambda}{\Lambda_H} \right)^2 \frac{m_b T_{\text{max}}^5}{H_{\text{inf}}} \exp \left[-\frac{2m_b}{T_{\text{max}}} \right], \quad (\text{A7})$$

where $n_{\text{eq}} = 4 \left(\frac{m_b T}{2\pi} \right)^{\frac{3}{2}} e^{-\frac{m_b}{T}}$ we used $m_b \gg T_{\text{reh}}$ limit and we have

$$\frac{a_{\text{inf}}}{a(t_0)} = \frac{a_{\text{inf}}}{a_{\text{reh}}} \frac{a_{\text{reh}}}{a(t_0)} = \left(\frac{\rho_{\text{reh}}}{\rho_{\text{inf}}} \right)^{\frac{1}{3(1+w)}} \left(\frac{g_{0,s}}{g_{\text{reh},s}} \right)^{\frac{1}{3}} \frac{T_0}{T_{\text{reh}}}. \quad (\text{A8})$$

Here T_0 is the temperature of the universe today and $g_{\text{reh},s}$ and $g_{0,s} = 3.91$ are the effective numbers of relativistic degrees of freedom contributing to the total entropy at reheating and today, respectively. The relic density of the dark baryons produced today through the Higgs portal is

$$\Omega_{b'} \equiv \frac{m_b n_b(t_0)}{\rho_{\text{crit}}} \approx \frac{5 \times 10^{10} / (2\pi)^4}{1+w} \frac{g_{0,s}}{g_{\text{reh},s}} \left(\frac{T_0}{T_{\text{reh}}} \right)^3 \left(\frac{\lambda}{\Lambda_H} \right)^2 m_b^2 \times (0.2)^{5 \frac{3}{8}} \frac{3.91}{100} (10\pi^2)^{1/(1+w)} \left(\frac{g_{\text{eff}}(T_{\text{reh}})}{100} \right)^{1/(w+1)-13/8} \times \frac{T_{\text{reh}}^{4/(1+w)+5/2}}{(M_{\text{pl}} H_{\text{inf}})^{2/(1+w)-1/4}} M_{\text{pl}} \exp \left[-\frac{2m_b}{T_{\text{max}}} \right] \text{eV}^{-4},$$

where $\rho_{\text{crit}} = 0.8 \times 10^{-10} \text{eV}^4$ is the total energy density of the universe today. In the case that $T_{\text{reh}} \gg T_{\text{EW}}$ and using the fact that $T_0 = 0.24 \times 10^{-3} \text{eV}$ and $M_{\text{pl}} = 2.4 \times 10^{18} \text{GeV}$, we have

$$\Omega_{b'} \approx \frac{5.6 \times 10^{15} (10\pi^2)^{\frac{-w}{(1+w)}}}{(2\pi)^2} \frac{(\lambda m_b)^2}{(1+w)} \left(\frac{T_{\text{reh}}^2}{M_{\text{pl}} H_{\text{inf}}} \right)^{\frac{2}{(1+w)} - \frac{1}{4}} \times \exp \left[-10 \left(\frac{m_b^2}{M_{\text{pl}} H_{\text{inf}}} \right)^{\frac{1}{2}} \left(\frac{M_{\text{pl}} H_{\text{inf}}}{T_{\text{reh}}^2} \right)^{\frac{1}{4}} \right]. \quad (\text{A9})$$

-
- [1] N. Aghanim *et al.* (Planck Collaboration), Planck 2018 results. VI. Cosmological parameters, *Astron. Astrophys.* **641**, A6 (2020).
- [2] E. G. M. Ferreira, Ultra-light dark matter, *Astron. Astrophys. Rev.* **29**, 7 (2021).
- [3] J. Preskill, M. B. Wise, and F. Wilczek, Cosmology of the invisible axion, *Phys. Lett.* **120B**, 127 (1983).
- [4] L. F. Abbott and P. Sikivie, A cosmological bound on the invisible axion, *Phys. Lett.* **120B**, 133 (1983).
- [5] M. Dine and W. Fischler, The not so harmless axion, *Phys. Lett.* **120B**, 137 (1983).
- [6] W. Hu, R. Barkana, and A. Gruzinov, Cold and Fuzzy Dark Matter, *Phys. Rev. Lett.* **85**, 1158 (2000).
- [7] L. Hui, J. P. Ostriker, S. Tremaine, and E. Witten, Ultra-light scalars as cosmological dark matter, *Phys. Rev. D* **95**, 043541 (2017).
- [8] C. G. Boehmer and T. Harko, Can dark matter be a Bose-Einstein condensate?, *J. Cosmol. Astropart. Phys.* **06** (2007) 025.
- [9] L. Berezhiani and J. Khoury, Theory of dark matter superfluidity, *Phys. Rev. D* **92**, 103510 (2015).
- [10] E. G. M. Ferreira, G. Franzmann, J. Khoury, and R. Brandenberger, Unified superfluid dark sector, *J. Cosmol. Astropart. Phys.* **08** (2019) 027.
- [11] S. Alexander and S. Cormack, Gravitationally bound BCS state as dark matter, *J. Cosmol. Astropart. Phys.* **04** (2017) 005.
- [12] S. Alexander, E. McDonough, and D. N. Spergel, Chiral gravitational waves and baryon superfluid dark matter, *J. Cosmol. Astropart. Phys.* **05** (2018) 003.
- [13] S. Alexander, E. McDonough, and D. N. Spergel, Strongly-interacting ultralight millicharged particles, *Phys. Lett. B* **822**, 136653 (2021).

- [14] J. S. Bullock and M. Boylan-Kolchin, Small-scale challenges to the λ cdm paradigm, *Annu. Rev. Astron. Astrophys.* **55**, 343 (2017).
- [15] S.-R. Chen, H.-Y. Schive, and T. Chiueh, Jeans analysis for dwarf spheroidal galaxies in wave dark matter, *Mon. Not. R. Astron. Soc.* **468**, 1338 (2017).
- [16] L. Berezhiani, B. Famaey, and J. Khoury, Phenomenological consequences of superfluid dark matter with baryon-phonon coupling, *J. Cosmol. Astropart. Phys.* **09** (2018) 021.
- [17] J. C. Niemeyer, Small-scale structure of fuzzy and axion-like dark matter, [arXiv:1912.07064](https://arxiv.org/abs/1912.07064).
- [18] D. Antypas *et al.*, New horizons: Scalar and vector ultralight dark matter, [arXiv:2203.14915](https://arxiv.org/abs/2203.14915).
- [19] T. Rindler-Daller and P. R. Shapiro, Angular momentum and vortex formation in bose-einstein-condensed cold dark matter haloes, *Mon. Not. R. Astron. Soc.* **422**, 135 (2012).
- [20] S. O. Schobesberger, T. Rindler-Daller, and P. R. Shapiro, Angular momentum and the absence of vortices in the cores of fuzzy dark matter haloes, *Mon. Not. R. Astron. Soc.* **505**, 802 (2021).
- [21] L. Berezhiani, G. Cintia, and M. Warkentin, Core fragmentation in simplest superfluid dark matter scenario, *Phys. Lett. B* **819**, 136422 (2021).
- [22] L. Hui, A. Joyce, M. J. Landry, and X. Li, Vortices and waves in light dark matter, *J. Cosmol. Astropart. Phys.* **01** (2021) 011.
- [23] S. Alexander, C. Capanelli, E. G. M. Ferreira, and E. McDonough, Cosmic filament spin from dark matter vortices, *Phys. Lett. B* **833**, 137298 (2022).
- [24] S. Alexander, S. Gleyzer, E. McDonough, M. W. Toomey, and E. Usai, Deep learning the morphology of dark matter substructure, *Astrophys. J.* **893**, 15 (2020).
- [25] P. Sikivie, N. Sullivan, and D. B. Tanner, Proposal for Axion Dark Matter Detection Using an LC Circuit, *Phys. Rev. Lett.* **112**, 131301 (2014).
- [26] P. Zyla *et al.* (Particle Data Group), Review of particle physics, *Prog. Theor. Exp. Phys.* **2020**, 083C01 (2020).
- [27] D. Croon, M. Gleiser, S. Mohapatra, and C. Sun, Gravitational radiation background from boson star binaries, *Phys. Lett. B* **783**, 158 (2018).
- [28] D. Croon, J. Fan, and C. Sun, Boson star from repulsive light scalars and gravitational waves, *J. Cosmol. Astropart. Phys.* **04** (2019) 008.
- [29] N. Kitajima, J. Soda, and Y. Urakawa, Nano-Hz Gravitational-Wave Signature from Axion Dark Matter, *Phys. Rev. Lett.* **126**, 121301 (2021).
- [30] C. S. Machado, W. Ratzinger, P. Schwaller, and B. A. Stefanek, Gravitational wave probes of axionlike particles, *Phys. Rev. D* **102**, 075033 (2020).
- [31] C. Yuan, R. Brito, and V. Cardoso, Probing ultralight dark matter with future ground-based gravitational-wave detectors, *Phys. Rev. D* **104**, 044011 (2021).
- [32] R. Janish and H. Ramani, Muon $g-2$ and EDM experiments as muonic dark matter detectors, *Phys. Rev. D* **102**, 115018 (2020).
- [33] A. Dev, P. A. N. Machado, and P. Martínez-Miravé, Signatures of ultralight dark matter in neutrino oscillation experiments, *J. High Energy Phys.* **01** (2021) 094.
- [34] Z. Bogorad and N. Toro, Ultralight millicharged dark matter via misalignment, *J. High Energy Phys.* **07** (2022) 035.
- [35] R. Garani, M. Redi, and A. Tesi, Dark QCD matters, *J. High Energy Phys.* **12** (2021) 139.
- [36] Y.-D. Tsai, R. McGehee, and H. Murayama, Resonant Self-Interacting Dark Matter from Dark QCD, *Phys. Rev. Lett.* **128**, 172001 (2022).
- [37] N. A. Dondi, F. Sannino, and J. Smirnov, Thermal history of composite dark matter, *Phys. Rev. D* **101**, 103010 (2020).
- [38] D. J. H. Chung, E. W. Kolb, and A. Riotto, Production of massive particles during reheating, *Phys. Rev. D* **60**, 063504 (1999).
- [39] D. J. H. Chung, E. W. Kolb, and A. Riotto, Nonthermal Supermassive Dark Matter, *Phys. Rev. Lett.* **81**, 4048 (1998).
- [40] V. Kuzmin and I. Tkachev, Matter creation via vacuum fluctuations in the early universe and observed ultrahigh-energy cosmic ray events, *Phys. Rev. D* **59**, 123006 (1999).
- [41] D. J. H. Chung, P. Crotty, E. W. Kolb, and A. Riotto, On the gravitational production of superheavy dark matter, *Phys. Rev. D* **64**, 043503 (2001).
- [42] D. Carney *et al.*, Snowmass2021 cosmic frontier white paper: Ultraheavy particle dark matter, [arXiv:2203.06508](https://arxiv.org/abs/2203.06508).
- [43] E. W. Kolb and A. J. Long, Completely dark photons from gravitational particle production during the inflationary era, *J. High Energy Phys.* **03** (2021) 283.
- [44] E. W. Kolb, A. J. Long, and E. McDonough, Catastrophic production of slow gravitinos, *Phys. Rev. D* **104**, 075015 (2021).
- [45] S. Alexander, L. Jenks, and E. McDonough, Higher spin dark matter, *Phys. Lett. B* **819**, 136436 (2021).
- [46] A. Malekenjad and E. McDonough, Longer Version (to be published).
- [47] J. M. Cline, Dark atoms and composite dark matter, *SciPost Phys. Lect. Notes* **52**, 1 (2022).
- [48] D. Feldman, Z. Liu, and P. Nath, The stueckelberg Z-prime extension with kinetic mixing and milli-charged dark matter from the hidden sector, *Phys. Rev. D* **75**, 115001 (2007).
- [49] P. J. Fox and E. Poppitz, Leptophilic dark matter, *Phys. Rev. D* **79**, 083528 (2009).
- [50] P. Fileviez Pérez, E. Golias, R.-H. Li, and C. Murgui, Leptophobic dark matter and the baryon number violation scale, *Phys. Rev. D* **99**, 035009 (2019).
- [51] M. Duerr, P. Fileviez Perez, and M. B. Wise, Gauge Theory for Baryon and Lepton Numbers with Leptoquarks, *Phys. Rev. Lett.* **110**, 231801 (2013).
- [52] E. Ma, Gauged baryon number and dibaryonic dark matter, *Phys. Lett. B* **813**, 136066 (2021).
- [53] S. Scherer and M. R. Schindler, A chiral perturbation theory primer, [arXiv:hep-ph/0505265](https://arxiv.org/abs/hep-ph/0505265).
- [54] B. Borasoy and S. Wetzel, U(3) chiral perturbation theory with infrared regularization, *Phys. Rev. D* **63**, 074019 (2001).
- [55] R. Kaiser and H. Leutwyler, Large N(c) in chiral perturbation theory, *Eur. Phys. J. C* **17**, 623 (2000).

- [56] M. D. Schwartz, *Quantum Field Theory and the Standard Model* (Cambridge University Press, Cambridge, England, 2014).
- [57] F. Close and P. R. Page, Glueballs, *Sci. Am.* **279**, 80 (1998).
- [58] G. S. Bali, K. Schilling, A. Hulsebos, A. C. Irving, C. Michael, and P. W. Stephenson (UKQCD Collaboration), A comprehensive lattice study of SU(3) glueballs, *Phys. Lett. B* **309**, 378 (1993).
- [59] A. Athenodorou and M. Teper, SU(N) gauge theories in $3 + 1$ dimensions: Glueball spectrum, string tensions and topology, *J. High Energy Phys.* **12** (2021) 082.
- [60] C. J. Morningstar and M. J. Peardon, The glueball spectrum from an anisotropic lattice study, *Phys. Rev. D* **60**, 034509 (1999).
- [61] Y. Chen *et al.*, Glueball spectrum and matrix elements on anisotropic lattices, *Phys. Rev. D* **73**, 014516 (2006).
- [62] M. Loan, X.-Q. Luo, and Z.-H. Luo, Monte Carlo study of glueball masses in the Hamiltonian limit of SU(3) lattice gauge theory, *Int. J. Mod. Phys. A* **21**, 2905 (2006).
- [63] H.-y. Jin and X.-m. Zhang, Scalar glueball decay into pions in effective theory, *Phys. Rev. D* **66**, 057505 (2002).
- [64] P. Asadi, E. D. Kramer, E. Kuflik, T. R. Slatyer, and J. Smirnov, Glueballs in a thermal squeezeout model, *J. High Energy Phys.* **07** (2022) 006.
- [65] D. J. E. Marsh, Axion cosmology, *Phys. Rep.* **643**, 1 (2016).
- [66] Y. Akrami *et al.* (Planck Collaboration), Planck 2018 results. X. Constraints on inflation, *Astron. Astrophys.* **641**, A10 (2020).
- [67] E. W. Kolb and A. J. Long, Superheavy dark matter through Higgs portal operators, *Phys. Rev. D* **96**, 103540 (2017).
- [68] M. Redi, A. Tesi, and H. Tillim, Gravitational production of a conformal dark sector, *J. High Energy Phys.* **05** (2021) 010.
- [69] D. J. H. Chung, E. W. Kolb, and A. J. Long, Gravitational production of super-Hubble-mass particles: An analytic approach, *J. High Energy Phys.* **01** (2019) 189.
- [70] Y. Ema, R. Jinno, K. Mukaida, and K. Nakayama, Gravitational effects on inflaton decay, *J. Cosmol. Astropart. Phys.* **05** (2015) 038.
- [71] Y. Ema, R. Jinno, K. Mukaida, and K. Nakayama, Gravitational particle production in oscillating backgrounds and its cosmological implications, *Phys. Rev. D* **94**, 063517 (2016).
- [72] Y. Ema, K. Nakayama, and Y. Tang, Production of purely gravitational dark matter, *J. High Energy Phys.* **09** (2018) 135.
- [73] Y. Ema, K. Nakayama, and Y. Tang, Production of purely gravitational dark matter: The case of fermion and vector boson, *J. High Energy Phys.* **07** (2019) 060.
- [74] N. Bar, K. Blum, and C. Sun, Galactic rotation curves versus ultralight dark matter: A systematic comparison with SPARC data, *Phys. Rev. D* **105**, 083015 (2022).
- [75] E. D. Schiappacasse and M. P. Hertzberg, Analysis of dark matter axion clumps with spherical symmetry, *J. Cosmol. Astropart. Phys.* **01** (2018) 037.
- [76] H.-K. Guo, K. Sinha, C. Sun, J. Swaim, and D. Vagie, Two-scalar Bose-Einstein condensates: From stars to galaxies, *J. Cosmol. Astropart. Phys.* **10** (2021) 028.
- [77] J. Eby, M. Leembruggen, L. Street, P. Suranyi, and L. C. R. Wijewardhana, Galactic condensates composed of multiple axion species, *J. Cosmol. Astropart. Phys.* **10** (2020) 020.
- [78] K. A. Oman *et al.*, The unexpected diversity of dwarf galaxy rotation curves, *Mon. Not. R. Astron. Soc.* **452**, 3650 (2015).
- [79] F. Lelli, S. S. McGaugh, and J. M. Schombert, SPARC: Mass models for 175 disk galaxies with spitzer photometry and accurate rotation curves, *Astron. J.* **152**, 157 (2016).
- [80] H. Y. J. Chan, E. G. M. Ferreira, S. May, K. Hayashi, and M. Chiba, The diversity of core-halo structure in the fuzzy dark matter model, *Mon. Not. R. Astron. Soc.* **511**, 943 (2022).
- [81] A. Berlin, R. T. D’Agnolo, S. A. R. Ellis, P. Schuster, and N. Toro, Directly Deflecting Particle Dark Matter, *Phys. Rev. Lett.* **124**, 011801 (2020).
- [82] C. Dvorkin, T. Lin, and K. Schutz, Making dark matter out of light: Freeze-in from plasma effects, *Phys. Rev. D* **99**, 115009 (2019).
- [83] K. K. Boddy, V. Gluscevic, V. Poulin, E. D. Kovetz, M. Kamionkowski, and R. Barkana, Critical assessment of CMB limits on dark matter-baryon scattering: New treatment of the relative bulk velocity, *Phys. Rev. D* **98**, 123506 (2018).
- [84] S. Davidson, S. Hannestad, and G. Raffelt, Updated bounds on millicharged particles, *J. High Energy Phys.* **05** (2000) 003.
- [85] G. G. Raffelt, *Stars as Laboratories for Fundamental Physics: The Astrophysics of Neutrinos, Axions, and Other Weakly Interacting Particles* (University of Chicago Press, 1996).
- [86] W. DeRocco, P. W. Graham, and S. Rajendran, Exploring the robustness of stellar cooling constraints on light particles, *Phys. Rev. D* **102**, 075015 (2020).
- [87] E. O. Nadler, V. Gluscevic, K. K. Boddy, and R. H. Wechsler, Constraints on dark matter microphysics from the Milky Way satellite population, *Astrophys. J. Lett.* **878**, L32 (2019).
- [88] N. Vinyoles and H. Vogel, Minicharged particles from the sun: A cutting-edge bound, *J. Cosmol. Astropart. Phys.* **03** (2016) 002.
- [89] M. Korwar and A. M. Thalappilil, Novel astrophysical probes of light millicharged fermions through schwinger pair production, *J. High Energy Phys.* **04** (2019) 039.
- [90] S. Davidson and M. E. Peskin, Astrophysical bounds on millicharged particles in models with a paraphoton, *Phys. Rev. D* **49**, 2114 (1994).
- [91] H. Vogel and J. Redondo, Dark Radiation constraints on minicharged particles in models with a hidden photon, *J. Cosmol. Astropart. Phys.* **02** (2014) 029.
- [92] C. Burrage, J. Jaeckel, J. Redondo, and A. Ringwald, Late time CMB anisotropies constrain mini-charged particles, *J. Cosmol. Astropart. Phys.* **11** (2009) 002.
- [93] M. Ahlers, H. Gies, J. Jaeckel, J. Redondo, and A. Ringwald, Laser experiments explore the hidden sector, *Phys. Rev. D* **77**, 095001 (2008).

- [94] A. Caputo, L. Sberna, M. Frias, D. Blas, P. Pani, L. Shao, and W. Yan, Constraints on millicharged dark matter and axionlike particles from timing of radio waves, *Phys. Rev. D* **100**, 063515 (2019).
- [95] M. Gluck, S. Rakshit, and E. Reya, The lamb shift contribution of very light milli-charged fermions, *Phys. Rev. D* **76**, 091701 (2007).
- [96] A. Badertscher, P. Crivelli, W. Fetscher, U. Gendotti, S. Gninenko, V. Postoev, A. Rubbia, V. Samoilenko, and D. Sillou, An improved limit on invisible decays of positronium, *Phys. Rev. D* **75**, 032004 (2007).
- [97] J. Jaeckel, Probing Minicharged Particles with Tests of Coulomb's Law, *Phys. Rev. Lett.* **103**, 080402 (2009).
- [98] H. Gies, J. Jaeckel, and A. Ringwald, Accelerator cavities as a probe of millicharged particles, *Europhys. Lett.* **76**, 794 (2006).
- [99] N. Aggarwal *et al.*, Challenges and opportunities of gravitational-wave searches at MHz to GHz frequencies, *Living Rev. Relativity* **24**, 4 (2021).
- [100] R. Khatriwada *et al.* (ADMX Collaboration), Axion dark matter experiment: Detailed design and operations, *Rev. Sci. Instrum.* **92**, 124502 (2021).
- [101] J. A. Dror, H. Murayama, and N. L. Rodd, Cosmic axion background, *Phys. Rev. D* **103**, 115004 (2021).
- [102] F. Finelli and M. Galaverni, Rotation of linear polarization plane and circular polarization from cosmological pseudo-scalar fields, *Phys. Rev. D* **79**, 063002 (2009).
- [103] M. P. Hertzberg and E. D. Schiappacasse, Dark matter axion clump resonance of photons, *J. Cosmol. Astropart. Phys.* **11** (2018) 004.